Osteoarthritis and Cartilage 19 (2011) 136–144

Osteoarthritis and Cartilage

OARSI OSTEOARTHRITIS RESEARCH SOCIETY INTERNATIONAL

Temporal and spatial modulation of chondrogenic foci in subchondral microdrill holes by chitosan-glycerol phosphate/blood implants

A. Chevrier †, C.D. Hoemann †‡, J. Sun §, M.D. Buschmann †‡*

† Department of Chemical Engineering, Ecole Polytechnique de Montreal, PO Box 6079, Succ Centre-Ville, Montreal, Quebec, Canada
‡ Institute of Biomedical Engineering, Ecole Polytechnique de Montreal, PO Box 6079, Succ Centre-Ville, Montreal, Quebec, Canada
§ Piramal Healthcare (Canada), Montreal, Quebec, Canada

ARTICLE INFO

Article history:
Received 15 June 2010
Accepted 26 October 2010

Keywords:
Cartilage repair
Bone repair
Chitosan
Chondrogenesis
Endochondral ossification

SUMMARY

Objective: Subchondral drilling initiates a cartilage repair response involving formation of chondrogenic foci in the subchondral compartment. The purpose of this study was to structurally characterize these sites of chondrogenesis and to investigate the effects of chitosan-glycerol phosphate (GP)/blood implants on their formation.

Method: Thirty-two New Zealand White rabbits received bilateral cartilage defects bearing four subchondral drill holes. One knee per rabbit was treated by solidifying a chitosan-GP/blood implant over the defect. After 1–56 days of repair, chondrogenic foci were characterized by histostaining and immunostaining. Collagen fiber orientation was characterized by polarized light microscopy.

Results: Glycosaminoglycan and collagen type II were present throughout the foci while the upper zone expressed collagen type I and the lower zone collagen type X. Large chondrogenic foci had a stratified structure with flatter cells closer to the articular surface, and round or hypertrophic chondrocytes deeper in the drill holes that showed signs of calcification after 3 weeks of repair in control defects. Markers for pre-hypertrophic chondrocytes (Patched) and for proliferation (Ki-67) were detected within foci. Some cells displayed a columnar arrangement where collagen was vertically oriented. For treated defects, chondrogenic foci appeared 1–3 weeks later, foci were nascent and mature rather than resorbing, and foci developed closer to the articular surface.

Conclusions: Chondrogenic foci bear some similarities to growth cartilage and can give rise to a repair tissue that has similar zonal stratification as articular cartilage. The temporal and spatial formation of chondrogenic foci can be modulated by cartilage repair therapies.

Introduction

Marrow-stimulation techniques such as abrasion arthroplasty[1], drilling[2] and microfracture[3] are clinically used treatments that take advantage of a natural repair response initiated by bone marrow-derived blood and cells. These methods aim to recruit and amplify bone marrow-derived mesenchymal stem cells (BMSCs) in the cartilage lesion[4]. Subsequently BMSCs must differentiate into chondrocytes in order to synthesize a cartilaginous repair tissue[4]. It is well established that *in vitro*, BMSC micromass cultures develop a cartilage matrix in chondrogenic media[5], through processes that partly recapitulate BMSC condensation and chondrogenesis in the embryonic limb bud[6]. Similarly, condensations of chondrocytes, referred to as "chondrogenic foci" in the remainder of this text, can be observed at intermediate stages of repair inside subchondral bone drill holes following marrow-stimulation treatments in animal models[7–17].

The induction of chondrogenic foci is not well documented or understood in the context of cartilage repair. Using a rabbit model of marrow stimulation, we hypothesized that the chondrogenic foci that form in subchondral drill holes display endochondral ossification characteristics. In the growth plate, the endochondral ossification processes of cell proliferation, enlargement, matrix synthesis followed by calcification, vascular invasion and synthesis of primary bone trabeculae all contribute to bone growth[18–21]. A similar endochondral growth process occurs at the surface of the developing epiphysis where immature articular cartilage functions as an articular-epiphyseal growth cartilage[22–24]. Fracture healing is yet another process that recapitulates certain aspects of skeletal development and growth[19,25,26], often proceeding through endochondral

* Address correspondence and reprint requests to: Michael D. Buschmann, Chemical Engineering Department, Ecole Polytechnique de Montreal, PO Box 6079, Succ Centre-Ville, Montreal, Quebec, Canada H3C 3A7. Tel: 1-514-340-4711x4931; Fax: 1-514-340-2980.
E-mail address: michael.buschmann@polymtl.ca (M.D. Buschmann).

1063-4584/$ – see front matter © 2010 Osteoarthritis Research Society International. Published by Elsevier Ltd. All rights reserved.
doi:10.1016/j.joca.2010.10.026

ossification. Indian hedgehog (Ihh) is one signaling molecule that regulates endochondral ossification[19] in the growth plate and developing articular surface[27] through a negative feedback loop with parathyroid hormone-related peptide (PTHrP) to control proliferation and maturation of the chondrocytes. Patched is one of many effectors of Ihh signaling in growth plate chondrocytes, acting as a receptor[28,29]. Since repair and regeneration can recapitulate certain developmental events, a detailed characterization of chondrogenic foci could improve understanding and development of new tissue engineering concepts for cartilage repair.

We have previously shown in a rabbit model that treating drilled cartilage defects with chitosan-glycerol phosphate (GP)/blood implants increases recruitment of host inflammatory and stromal cells as well as subchondral vascularization, bone remodeling and improves cartilage repair[14–17]. Chondrogenic foci formed at 2–5 weeks post-operative in the subchondral space appeared to be the origin of cartilaginous repair tissues in animal models of marrow stimulation[14–17] but they have only been partly characterized to date. Therefore, the purpose of this study was to characterize chondrogenic foci that are induced in the subchondral granulation tissue following marrow-stimulation procedures, with and without treatment with chitosan-GP/blood implants. We tested the hypotheses that chondrogenic foci would contain stratified layers of cells expressing proliferation and chondrogenesis markers in distinct zones, and that their appearance would be modified both spatially and temporally by the treatment. Using a previously developed rabbit model[14,16,17], bilateral trochlear cartilage defects were drilled, and one defect was further treated with a chitosan-GP/blood implant. Animals were left to heal for time points ranging from 1 to 56 days post-surgery. Chondrogenic foci were categorized as nascent, mature or resorbing based on global morphology, while the timing of foci appearance and foci position relative to the articular surface were recorded. Chondrogenic foci were also characterized using glycosaminoglycan (GAG) histostaining, collagens type II, I, and X immunostaining and collagen structure through polarized light microscopy (PLM). Patched immunostaining was used to identify pre-hypertrophic chondrocytes and Ki-67 immunostaining was used to identify proliferating cells.

Materials and methods

Rabbit cartilage repair model

Skeletally mature New Zealand White (NZW) rabbits (Charles River, St. Constant, QC, Canada) housed individually in cages were used for this trochlear cartilage repair study (Table I). The housing, care and study protocol were approved by the Animal Care Committee of the University of Montreal. The animals were randomized according to sex and weight for distribution to treatment group and to each time point. The treated knee (left or right) was also randomized. Trochlear full-thickness chondral defects of 3.5 mm × 4.5 mm were created by using 1.5 mm and 2.75 mm flat blades (10035-05 and 10035-10, Fine Science Tools, North Vancouver, BC, Canada) and an arthrotomy technique. Four drill holes of ~4 mm depth were then perforated into the subchondral bone in each of the four corners of the defect using a high-speed microdrill (18000-17, Fine Science Tools, North Vancouver, BC, Canada) and a 0.9 mm-diameter drill bit (19007-21, Fine Science Tools, North Vancouver, BC, Canada). Continuous irrigation with cooled phosphate buffered saline (PBS) was used to limit thermal necrosis[30]. No antibiotics were administered at any time and all animals were allowed unrestricted ambulation post-surgery. Additionally, intact tibial growth plates and trochlear articular cartilage were collected from three young (3 months old) New Zealand White (NZW) rabbits (Table I).

Table I
Number of animals evaluated in each group at each time point

Group	Cartilage repair*	Unoperated†
Age	8–15 months	3 months
Average weight	4.8 kg	1.9 kg
Sacrifice at day 0	–	3 females
Sacrifice at day 1	2 Males, 3 females	–
Sacrifice at day 3	3 Males, 2 females	–
Sacrifice at day 7	2 Males, 3 females	–
Sacrifice at day 14	4 Males, 4 females	–
Sacrifice at day 21	2 Males, 1 females	–
Sacrifice at day 35	1 Males, 2 females	–
Sacrifice at day 56	2 Males, 1 females	–
Total	32	3

* All femurs in this group were processed for cryosectioning.
† Two femurs in this group were processed for paraffin sectioning, the rest were cryosectioned.

Preparation and application of chitosan-GP/blood implants

Chitosan powder with 77–83% degree of deacetylation was obtained from Piramal Healthcare (Canada), Montreal, QC Canada (formely BioSyntech Inc). Sterile chitosan-GP solutions were prepared as previously described[14], with 1.5% or 1.7% (w/v) chitosan, 135 mM disodium β-glycerophosphate, 59 mM HCl (pH 6.75–6.82 and osmolality 444–520 mOsm/kg) flash-frozen, stored in sterile glass vials at −80°C, and thawed the day of surgery. 3.5 ml of autologous blood was aseptically withdrawn from the rabbit ear artery and added to the vial containing 1.18 ml sterile chitosan-GP solution. The vial contained six sterile surgical stainless steel beads (0.39 g each, #9736, Salem Specialty Ball Co, Canton, CT, USA) and was shaken vigorously by hand for 10 s for mixing. A 3 cc syringe equipped with an 18 gauge needle was used to withdraw approximately 3 ml of the chitosan-GP/blood solution and one hanging drop of this solution was applied to the drilled cartilage defect. Coagulation was allowed for 5–8 min before closing the knee.

Histostaining, histomorphometry and PLM

Following decalcification, femurs were processed for cryosectioning as previously described[31] or for paraffin embedding and sectioning (Table I). All reagents were obtained from Sigma–Aldrich (Oakville, ON, Canada) unless otherwise specified. Sections taken from the middle of the proximal holes and of the distal holes were sequentially immersed in Weigert iron hematoxylin (HT-1079), 0.04% (w/v) Fast Green (F-7252) and 0.1% (w/v) Safranin O (S-2255) in water. Safranin O/Fast Green-stained sections were digitized at 40× magnification using a Nanozoomer RS slide scanner (Olympus, Markham, ON, Canada). The maturity of each chondrogenic foci within the subchondral soft repair tissue in the proximal and distal holes was established using the following criteria: Nascent foci were small (<0.1 mm^2) with a relatively homogenous cell population and matrix. Mature foci were larger and displayed a more stratified structure with flatter cells towards the articular surface and round, polygonal or hypertrophic cells underneath. Resorbing foci were identified by extensive vascular invasion and endochondral ossification from the bottom up. With the Safranin O-Fast Green-stained sections, the area (mm^2) of each foci was obtained by manually tracing around the Safranin O+ foci using NDPview software (Olympus, Markham, ON, Canada). The location of foci was characterized using line tracing in NDPview software to measure the distance (μm) between the top of a drill hole and the top of each foci. PLM observations were performed by adding a polarizer and Zeiss

453685 analyzer filter to a Zeiss Axiolab microscope equipped with a digital Hitachi HV-F22F camera.

Collagen immunostaining

Sections were subjected to antigen retrieval by heating in 10 mM Tris pH 10. Enzymatic treatment was with 0.25% (w/v) trypsin (EC 3.4.21.4) (Sigma Product No. T-8802) or 0.1% (w/v) pronase (EC 3.4.24.31) (P-8811) and 2.5% (w/v) hyaluronidase (EC 3.2.1.35) (H-3506). Sections were blocked with 20% (v/v) goat serum (G-9023) in PBS with 0.1% Triton X-100 (T-8532) for 60 min at room temperature and incubated with the primary antibody of interest diluted with 10% goat serum/PBS/0.1% triton X-100 for 60 min at room temperature or overnight at 4°C. Primary antibodies included monoclonal anti-collagen type I clone COL-1 (C-2456), monoclonal anti-collagen type I clone I-8H5 (631701, MP Biomedicals, Montreal, QC, Canada), monoclonal anti-collagen type II (II-II6B3, DSHB, Iowa, USA) and monoclonal anti-collagen type X clone COL-10 (C-7974). Sections were incubated with biotinylated goat anti-mouse IgG (Fab specific) (B-7151) diluted with 10% goat serum in PBS with 0.1% triton X-100 for 60 min at room temperature. Histochemical detection was performed with the Vectastain ABC-Alkaline Phosphatase (AP) system and AP Red Substrate kit (AK-5000 and SK-5100, Vector Laboratories Inc, Burlington, ON, Canada).

Patched and Ki-67 immunostaining

Sections were subjected to enzymatic digestion with 0.25 U/ml chondroitinase ABC (EC 4.2.2.4) (C-2905), then antigen retrieval by heating in 10 mM sodium citrate pH 6.1. Endogenous peroxidase was blocked by incubating in 3% H_2O_2 (5155-01, JT Baker, Phillipsburg, NJ, USA). Blocking was with 3% bovine serum albumin (BSA) (A-7888) and 5% milk powder in PBS for 60 min at room temperature. Primary antibodies diluted in 1% BSA/PBS were incubated overnight at 4°C with: monoclonal anti-Ki-67 Clone MIB-1 (M7240, Dako, Mississauga, ON, Canada) or monoclonal anti-Patched (Apa-1, DSHB, Iowa, USA). Sections were incubated with biotinylated goat anti-mouse IgG (Fab specific) (B-7151) diluted with 1% BSA in PBS for 60 min at room temperature. Histochemical detection was performed with the Vectastain ABC-peroxidase system (PK-6200, Vector Laboratories Inc, Burlington, ON, Canada) and DAB substrate kit (00-2020, Zymed, Burlington, ON, Canada).

Statistical analyses

The General Linear Model and analysis of variance (ANOVA) (Statistica version 6.1, Statsoft Inc, Tulsa, OK, USA) were used to analyze the effect of treatment on foci categorization (nascent, mature or resorbing) using day as co-variate. The two-tailed *t*-test

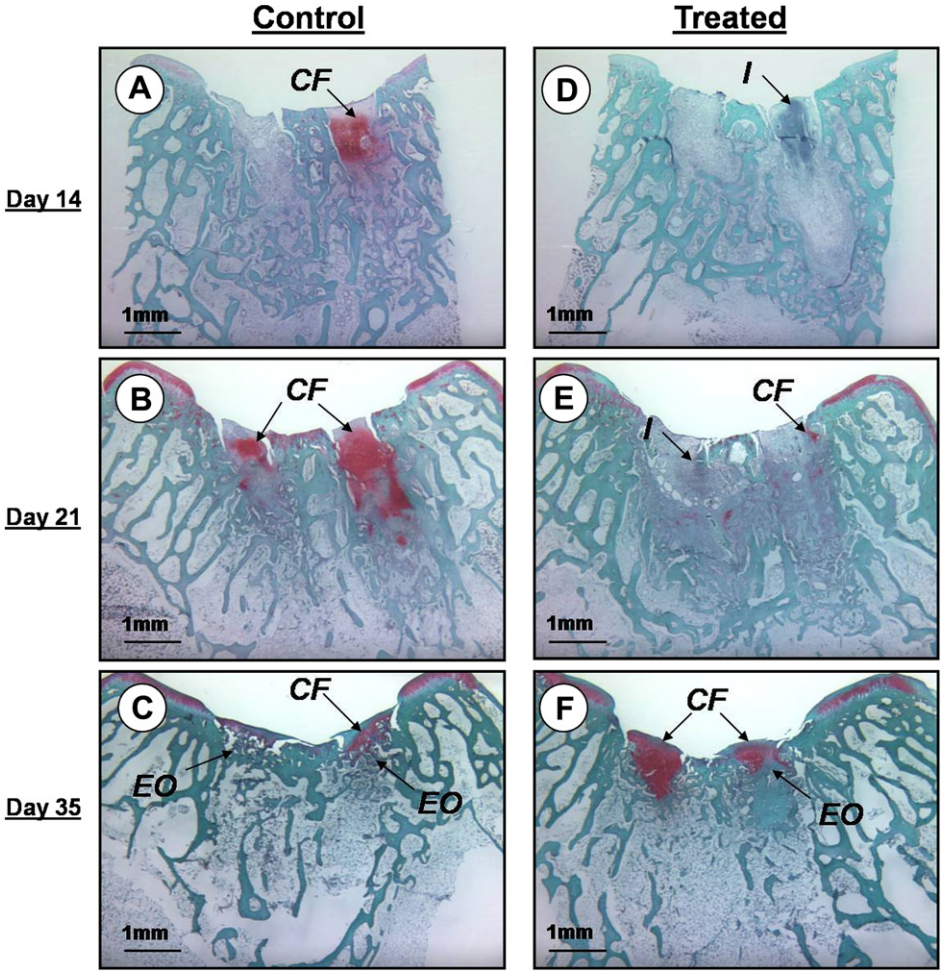

Fig. 1. Safranin O/Fast Green-stained sections from repairing cartilage defects at 14 (A&D), 21 (B&E) and 35 (C&F) days post-surgery. Chondrogenic foci (*CF* in A–C) were observed in control drill holes from 14 days on. Treatment with the chitosan-GP/blood implant (*I* in D&E) delayed the appearance of chondrogenic foci to 21 days post-treatment (*CF* in E). Vascular invasion and endochondral ossification were observed at later times (*EO* in C&F).

was used to test whether treatment displaced chondrogenic foci towards the articular surface. $P < 0.05$ was considered significant.

Results

Chitosan-GP/blood implants delay chondrogenic foci formation to 21 days post-treatment vs 14 days for controls

In the control drill holes, blood clot formation was followed by inflammatory and marrow-derived stromal cell migration, synthesis of granulation tissue and chondrogenic foci formation, starting at 2 weeks post-operative (Fig. 1). Chondrogenic foci were observed in 38% of control drill holes at 14 days and in 83% of control drill holes at 21 days [*CF* in Fig. 1(A&B)]. At 35 days, chondrogenic foci were present in 92% of control drill holes. Chondrogenic foci were growing above the tidemark in flanking cartilage to become cartilaginous repair tissues and most were being resorbed from below by the endochondral ossification process [*CF* and *EO* in Fig. 1(C)].

In the treated drill holes, the chitosan-GP/blood implant [*I* in Fig. 1 (D&E)] was histologically detectable until 21 days post-treatment. As previously described[14], chitosan-GP/blood implants increased recruitment of inflammatory cells and marrow-derived stromal cells during this period, and induced angiogenesis and bone remodeling under treated defects. Chitosan-GP/blood implants also delayed chondrogenic foci formation during the 14–21 day post-treatment period as only 2% of treated drill holes contained chondrogenic foci at these time points [*CF* in Fig. 1(E)]. In contrast, at 35 days, 83% of treated drill holes had chondrogenic foci, with fewer foci compared to control being resorbed from below through endochondral ossification [*CF* and *EO* in Fig. 1(F)].

Chondrogenic foci display different morphologies

Chondrogenic foci displayed distinct morphologies that we classified as nascent, mature or resorbing, as described in the Methods section. Cartilage differentiation was initiated in close proximity with bone as nearly all nascent foci were found at the edges of the drill holes (Fig. 2). The matrix of the small nascent foci (days 14–21 in control and days 21–35 in treated drill holes) contained a relatively homogenous cell population, GAG and collagen type II throughout [Fig. 2(A&B, E&F)]. Collagen type I also was present throughout the matrix in 12 out of 14 nascent foci [Fig. 2(C)].

All of the larger and more mature chondrogenic foci (days 14–35 in control and day 35 in treated drill holes) displayed a more evident stratified zonal structure with spatially dependent cell morphologies and matrix composition. In top regions closest to the articular surface, cells with flat, polygonal or round morphology were surrounded by a matrix containing GAG, collagen type II and collagen type I (region 1 in Fig. 3). At the bottom of the foci facing the subchondral bone, the cells were round, the matrix was rich in GAG and collagen type II, and some chondrocytes were undergoing hypertrophy coincident with collagen type X immunostaining (region 2 in Fig. 3). Chondrogenic foci were disorganized compared to the stratified organization of the growth plate and developing cartilage[20–24], where distinct regions of pre-hypertrophic chondrocytes (Patched+) were observed above hypertrophic chondrocytes (collagen type X+) at the surface of the developing epiphysis and in the growth plate (results not shown).

Extensive vascular invasion and endochondral ossification were visible at the bottom of resorbing foci (days 21–35 in control and day 35 in treated drill holes) (Fig. 4). In all resorbing foci, GAG and collagen type II co-localized [Fig. 4(A&B, E&F)] and some cells were undergoing hypertrophy as indicated by the expression of collagen type X [Fig. 4(D&H)]. There was a layer of collagen type I positive tissue directly above the GAG-rich tissue in 14 out of 15 resorbing foci [Fig. 4(C&G)].

The timing and location of chondrogenic foci are modulated by chitosan-GP/blood implants

Treatment with chitosan-GP/blood implants delayed the appearance of the nascent chondrogenic foci to 21 days compared

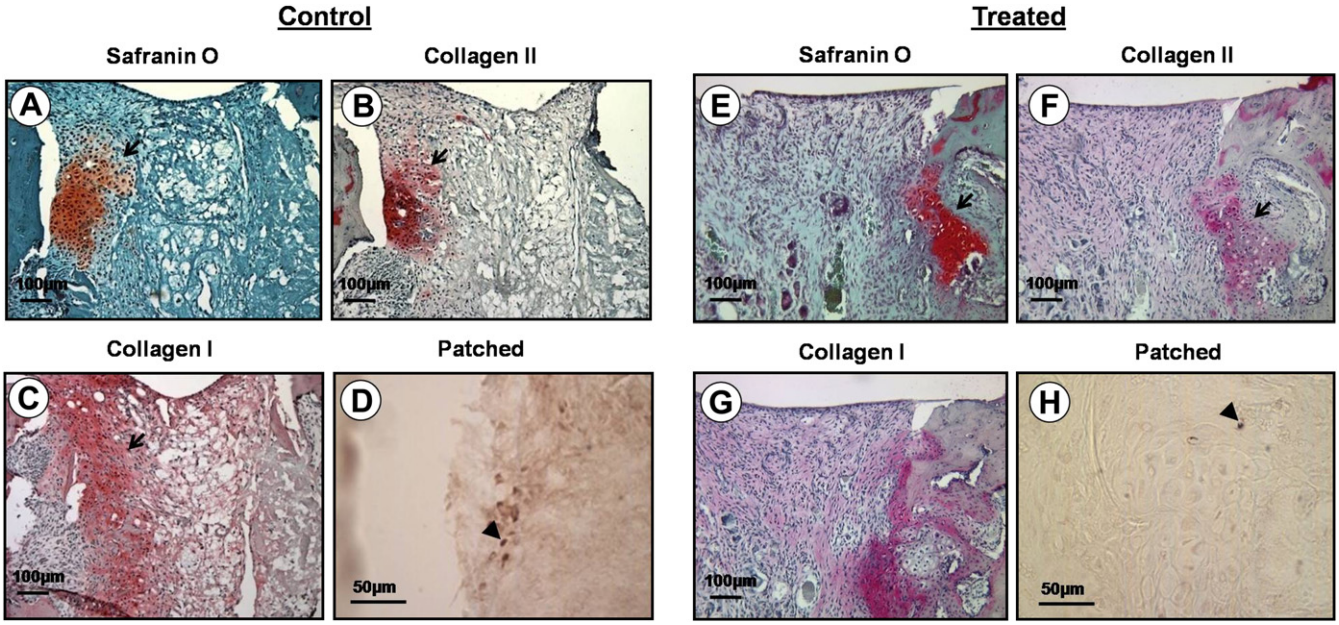

Fig. 2. Small nascent foci (black arrows) first occurred at day 14 in controls (A–D) and day 21 in treated drill holes (E–H) and contained a relatively homogenous cell population and expressed GAG (A&E) and collagen type II (B&F) throughout. Collagen type I was also present throughout in 12 nascent foci out of 14 (C). Some cells in nascent foci were committed to the chondrocyte lineage and pre-hypertrophic as shown by Patched immunostaining (D&H).

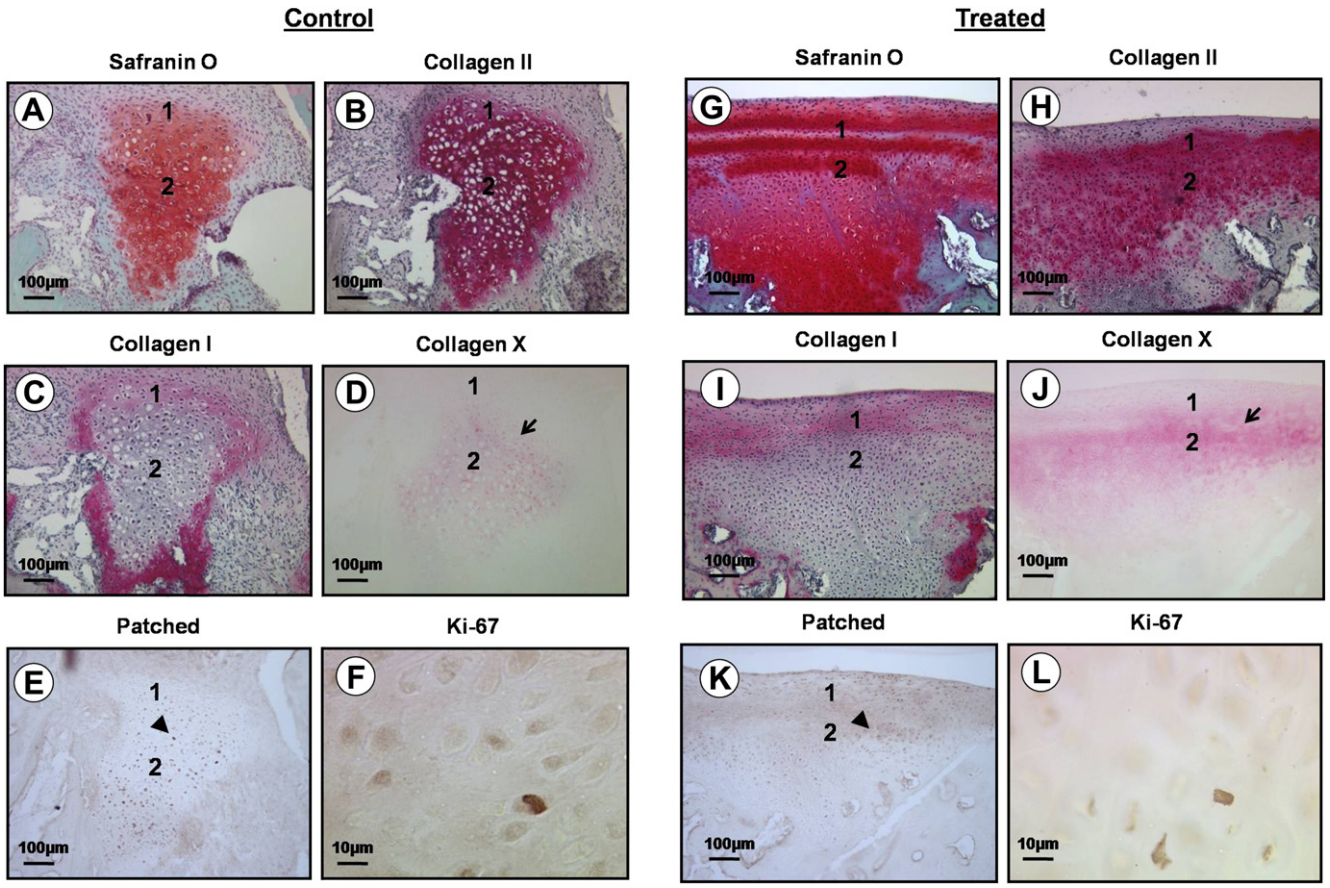

Fig. 3. The more mature foci first occurred at day 14 in controls (A–F) and day 35 in treated drill holes (G–L) and were arranged in two distinct zones. In the upper region closest to the articular surface (1), cells were flat, polygonal or round and were surrounded by a matrix containing GAG, collagen type II and collagen type I. At the bottom of the foci facing the subchondral bone (2), the cells were round and the matrix was rich in GAG and collagen type II. Several chondrocytes within the lower region showed signs of hypertrophy coincident with collagen type X immunostaining (arrows in D&J) while others were at an earlier differentiation stage as indicated by Patched immunostaining (arrowheads in E&K). Proliferating cells were identified by Ki-67 immunostaining within the foci (F&L).

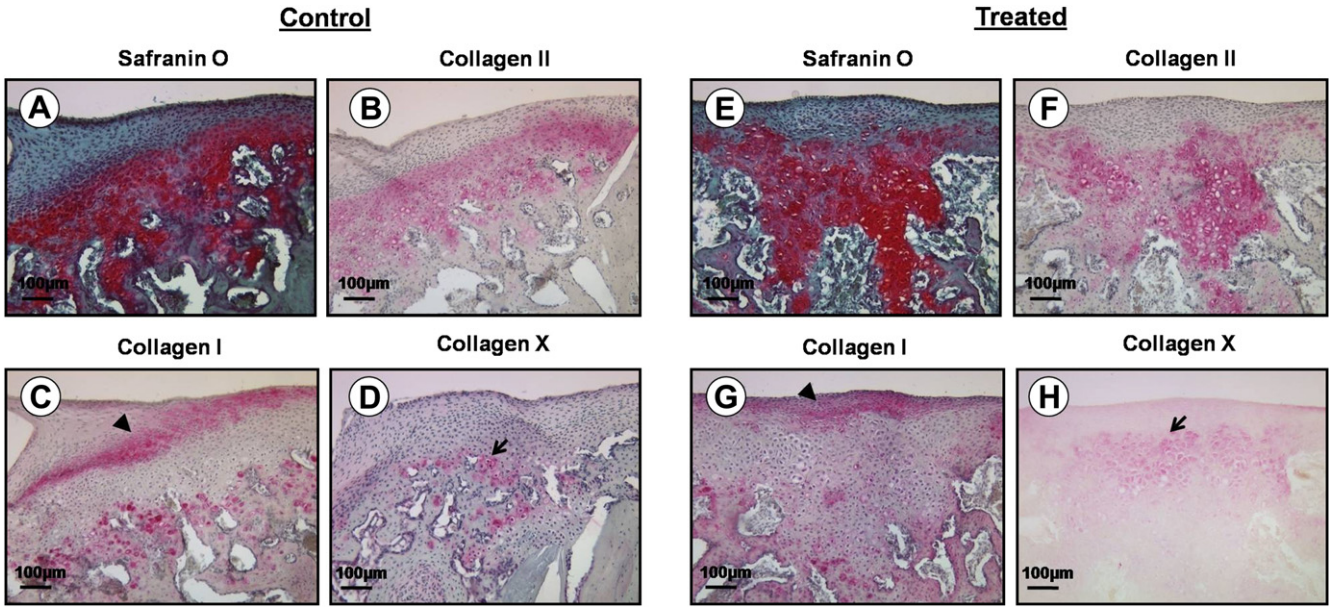

Fig. 4. Resorbing chondrogenic foci in control (A–D, day 35) and treated drill holes (E–H, day 35) stained for GAG (A&E) and collagen type II (B&F). Extensive vascular invasion and endochondral ossification were observed at the bottom of the foci (A&E). Some cells were undergoing hypertrophy as shown by collagen type X immunostaining (black arrows in D&H). A layer of collagen type I immunopositive tissue was observed above the foci (black arrowheads in C&G).

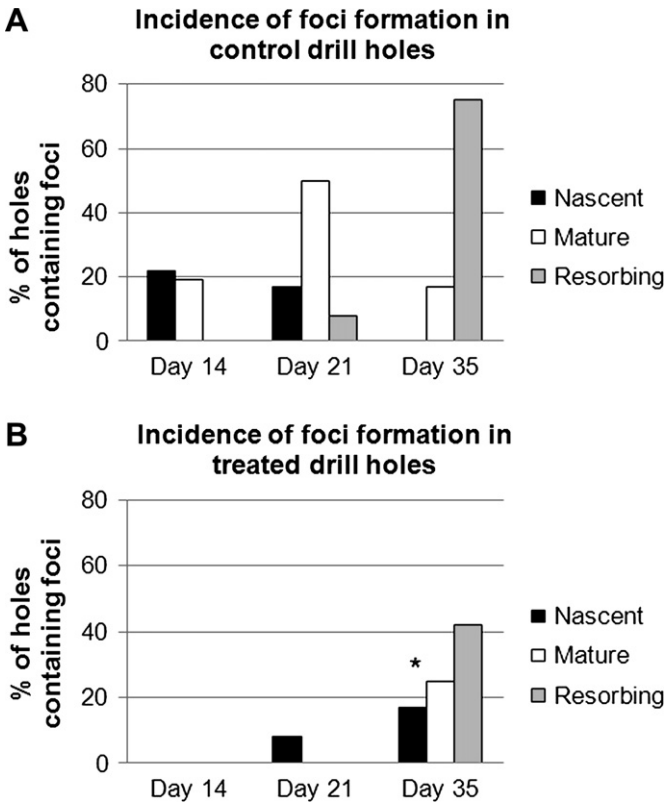

Fig. 5. Incidence of foci formation in the drill holes at different time points. Data is presented as the % of holes containing foci at day 14 for eight animals (32 holes per treatment) and at days 21 and 35 for three animals (12 holes per treatment). Chitosan-GP/blood implants delayed the appearance of nascent chondrogenic foci to 21 days in treated drill holes (B) vs 14 days in control drill holes (A). Mature chondrogenic foci mainly appeared at 35 days in treated drill holes (B) vs at 21 days in control drill holes (A). * Treatment led to a significant switch from resorbing foci in controls to nascent and mature foci in treated defects using the General Linear Model with day as co-variate ($P = 0.0064$) as well as with ANOVA on day 35 alone ($P = 0.040$).

to 14 days in the control drill holes (compare A and B in Fig. 5). Furthermore, mature foci formation was delayed to 35 days in the treated drill holes compared to 14 days in the controls (Fig. 5). By 35 days, most foci (9 out of 11) in the control drill holes were resorbing [Fig. 5(A)]. In treated drill holes at day 35, only 5 of 11 were resorbing [Fig. 5(B)]. Foci maturation and ossification were significantly delayed by treatment ($P = 0.0064$), and significantly more nascent and mature foci were present in treated drill holes at day 35 ($P = 0.040$). Treatment also moved nascent and mature chondrogenic foci towards the articular surface according to measured distances at the different time points. Overall, the average distance between the top of the drill holes and the top of nascent and mature chondrogenic foci was greater in control drill holes when compared to treated drill holes ($P = 0.029$ for nascent foci and $P = 0.01$ for mature foci) (Fig. 6). The distance from the surface for resorbing foci was not significantly different between treated and control drill holes (Fig. 6).

Chondrogenesis and cell proliferation markers are detected in foci

Nascent [Fig. 2(D&H)], mature [Fig. 3(E&K)] and resorbing foci all contained Patched+ cells throughout the foci, except in two mature foci from the control group, where Patched+ cells were found strictly above a layer of hypertrophic cells expressing collagen type X, in a manner similar to that observed in the growth plate (results not shown). All mature [Fig. 3(F&L)] and resorbing foci

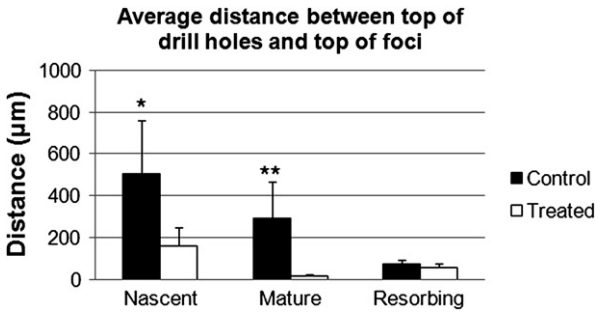

Fig. 6. The average distance between the top of the drill holes and the top of the chondrogenic foci in control vs treated drill holes. Data is presented as the mean with error bars representing the 95% confidence intervals. $n = 10$, 15, 10 and 4, 3, 5 for nascent, mature and resorbing foci in control and treated drill holes respectively. At 35 days, a total of 11 foci were observed in both control and treated drill holes. Treatment delayed and displaced chondrogenic foci towards the articular surface. $^{*}P = 0.029$ for nascent foci and $^{**}P = 0.01$ for mature foci comparing control vs treated with two-tailed t-test.

contained Ki-67+ proliferating cells, throughout the foci, in contrast to growth plate cartilages which have a restricted proliferative zone[20,21]. By 35 days post-treatment, all mature and resorbing foci were growing above the tidemark in flanking cartilage and the cartilaginous repair tissue in the chondral zone contained Patched and Ki-67 immunopositive cells.

Columnar cell organization and collagen fiber alignment are observed in the foci

PLM showed that collagen was oriented either vertically, horizontally or oblique to the surface of the drill hole in 10 nascent foci while four nascent foci had no discernable collagen orientation. In the deeper region of 15 out of 18 mature foci, some cells were aligned in short vertical columns of 2–9 cells surrounded by a matrix with vertically oriented collagen fibers [black arrows in Fig. 7(B&D)]. These structures were strikingly similar to the deep zone (DZ) of articular cartilage with columnar cells and vertically organized fibers that are essential to anchor the cartilage layer to subchondral bone. At the top of 8 out of 18 mature foci, closer to the articular surface, collagen fibers were parallel to the articular surface and contained flattened cells [white arrows in Fig. 7(B&D)]. Altogether, these data suggest that during a 3-week repair period (2–5 weeks), chondrogenic foci had the propensity to develop an appropriately stratified collagen network with horizontal fibers at the articular surface arcading to vertical fibrils in deeper zones.

Discussion

The objective of this study was to characterize chondrogenic foci that occur in subchondral tissues following bone marrow-stimulation procedures. Our results revealed that chondrogenic foci have the propensity to develop a stratified zonal structure similar to growth plate and developing articular cartilage, but that expression of chondrogenesis markers and cell proliferation occurs in a less organized manner. Treatment with chitosan-GP/blood implants did not appear to significantly alter the structural organization of chondrogenic foci, but rather changed their timing, maturation and position relative to the articular surface.

The delay in chondroinduction in treated drill holes may be directly related to the previously reported increase in blood vessel density under defects treated with chitosan-GP/blood implants[14–17] during the 21 day period in which the implant is present. The presence of a large number of blood vessels in the drill holes may for example delay chondroinduction in treated defects since low

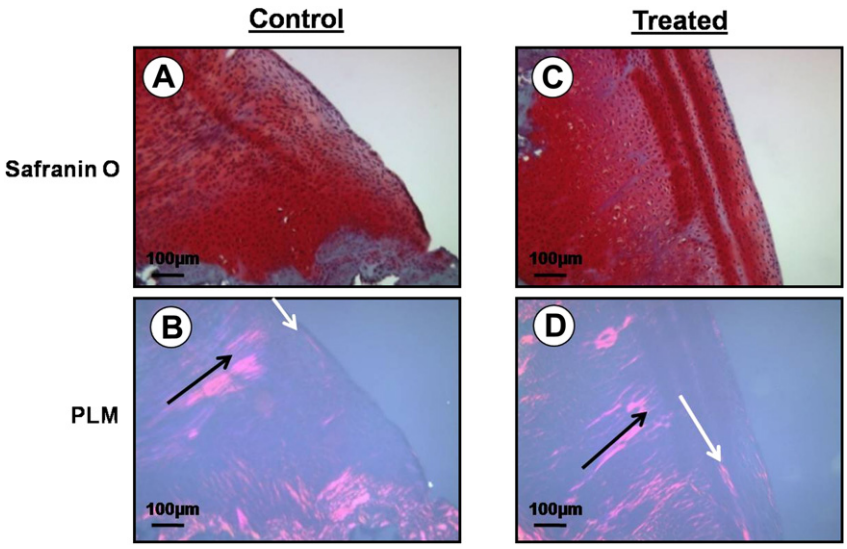

Fig. 7. Mature chondrogenic foci from control (A–B) and treated drill holes (C–D) stained with Safranin O-Fast Green and observed with PLM. Some cells from the deeper zones were arranged in short vertical columns and their collagen structure was arranged in a vertical orientation (black arrows in B&D). In mature foci, some cells from the superficial zones displayed a flattened morphology where some collagen fibers were also aligned parallel to the surface (white arrows in B&D).

oxygen tension has been shown to induce chondrogenesis of mesenchymal cells *in vitro*[32]. A major difference between cartilage formation during development and cartilage formation in the context of repair and regeneration is the significant role of inflammation in the healing process. We have previously shown that more neutrophils and alternatively activated macrophages populate the drill hole granulation repair tissues below chitosan implants[14,17]. These cells can secrete cytokines and growth factors that modulate the healing sequence. Inflammation has been suggested to be involved in the delay of callus formation in fracture repair models[33,34]. In the context of skin wound healing, it has been proposed[35] that the rapid synthesis of connective tissue hinders tissue regeneration and that slowing the repair process could allow regeneration by progenitor cells rather than scar formation. The effects of treatment observed here where chondrogenic foci occur closer to the articular surface and are shifted from resorbing to nascent and mature foci are expected to improve chondral resurfacing. Induction of chondrogenic foci closer towards the articular surface could reestablish a more durable and continuous layer of columnar and hyaline chondral repair tissue which more closely resembles articular cartilage, as we have previously shown in the rabbit and in the sheep[15–17].

As expected, we found that Patched and Ki-67 immunostaining in the growth plate and developing articular cartilage was zone-dependant. In contrast, in most mature chondrogenic foci, Patched, Ki-67 and collagen type X expression was overlapping in the lower region, indicating that foci were composed of a mixed cell population differentiated to different degrees. As is seen in fracture callus[36], the general fate of foci with ubiquitous collagen type X distribution was to ossify in deeper zones. Although we have not previously observed this in our rabbit and sheep models at 2 and 6 months of healing, bone overgrowth into the chondral compartment is an important concern in marrow-stimulation procedures[37,38]. Bone overgrowth following microfracture and debridement could be the result of uncontrolled calcification of foci that express collagen type X in the newly formed cartilaginous layer. Treatments that induce foci with a stratified organization that prevents induction of collagen type X in the superficial layer would be expected to suppress the tendency for bone overgrowth and could prove beneficial in the longer term in this respect. Chondrogenic foci do possess the ability to develop a stratified structure similar to growth cartilages: In two mature foci, a layer of pre-hypertrophic Patched+ cells was found strictly above hypertrophic cells expressing collagen type X, however events that led to this superior stratification are still unknown at this point. One limitation of the current study was the limited number of defects available at day 35 and more defects should be generated around this time point to better understand the frequency of stratified foci induction due to treatment.

In summary, chondrogenic foci arising in cartilage repair from subchondral bone marrow stimulation bear some structural similarities to growth plate and developing articular cartilage in terms of cell morphology, the patterning of collagens type I, II, X and the signals that regulate chondrocyte differentiation, maturation and proliferation, but they display a less stratified structure and lower degree of organization. We have previously shown that applying chitosan-GP/blood implants to marrow-stimulated cartilage defects improves the hyaline quality of the cartilage repair tissue[15–17]. Here we show that this improved outcome is partly related to a delayed appearance of foci towards the articular surface and a reduction of the appearance of resorbing foci. Cartilage repair therapies that produce a coordinated induction of chondrogenic foci and controlled appositional growth closer towards the articular surface could improve functional outcomes.

Contributions

The authors made substantial contributions in designing the study (AC, CDH, MDB), gathering and analyzing the data (AC, CHD, JS, MDB) and drafting the article (AC, CDH, MDB).

Competing interest

In support of this research, one or more of the authors received grants or outside funding from BioSyntech, Inc. No commercial entity paid or directed any benefits to any research fund, foundation, educational institution, or other nonprofit organization with which the authors are affiliated.

Acknowledgements

Financial support was provided by the Canadian Institutes of Health Research (CIHR), the Canada Research Chairs program

(MDB) and the Canada Foundation for Innovation (CFI). Salary support for CDH was provided by the Fonds de la Recherche sur la Santé du Québec (FRSQ).

References

1. Johnson LL. Arthroscopy abrasion arthroplasty. In: Operative Arthroscopy. 2nd edn. Philadelphia: Lippincott-Raven Publishers; 1996:341–60.
2. Insall J. The Pridie debridement operation for osteoarthritis of the knee. Clin Orthop 1974;101:61–7.
3. Steadman JR, Rodkey WG, Rodrigo JJ. Microfracture: surgical technique and rehabilitation to treat chondral defects. Clin Orthop 2001;391(Suppl):S362–9.
4. Richter W. Mesenchymal stem cells and cartilage in situ regeneration. J Intern Med 2009;266(4):390–405.
5. Johnstone B, Hering TM, Caplan AI, Goldberg VM, Yoo JU. In vitro chondrogenesis of bone marrow-derived mesenchymal progenitor cells. Exp Cell Res 1998;238(1):265–72.
6. Sekiya I, Vuoristo JT, Larson BL, Prockop DJ. In vitro cartilage formation by human adult stem cells from bone marrow stroma defines the sequence of cellular and molecular events during chondrogenesis. Proc Natl Acad Sci U S A 2002;99(7): 4397–402.
7. Meachim G, Roberts C. Repair of the joint surface from subarticular tissue in the rabbit knee. J Anat 1971;109:317–27.
8. Mitchell N, Shepard N. The resurfacing of adult rabbit articular cartilage by multiple perforations through the subchondral bone. J Bone Joint Surg Am 1976;58:230–3.
9. Shapiro F, Koide S, Glimcher MJ. Cell origin and differentiation in the repair of full-thickness defects of articular cartilage. J Bone Joint Surg Am 1993;75:532–53.
10. Mizuta H, Kudo S, Nakamura E, Otsuka Y, Takagi K, Hiraki Y. Active proliferation of mesenchymal cells prior to the chondrogenic repair response in rabbit full-thickness defects of articular cartilage. Osteoarthritis Cartilage 2004;12(7): 586–96.
11. Mizuta H, Kudo S, Nakamura E, Takagi K, Hiraki Y. Expression of the PTH/PTHrP receptor in chondrogenic cells during the repair of full-thickness defects of articular cartilage. Osteoarthritis Cartilage 2006;14(9):944–52.
12. Anraku Y, Mizuta H, Sei A, Kudo S, Nakamura E, Senba K, *et al*. The chondrogenic repair response of undifferentiated mesenchymal cells in rat full-thickness articular cartilage defects. Osteoarthritis Cartilage 2008;16(8):961–4.
13. Anraku Y, Mizuta H, Sei A, Kudo S, Nakamura E, Senba K, *et al*. Analyses of early events during chondrogenic repair in rat full-thickness articular cartilage defects. J Bone Miner Metab 2009;27(3):272–86.
14. Chevrier A, Hoemann CD, Sun J, Buschmann MD. Chitosan-glycerol phosphate/blood implants increase cell recruitment, transient vascularization and subchondral bone remodeling in drilled cartilage defects. Osteoarthritis Cartilage 2007;15 (3):316–27.
15. Hoemann CD, Hurtig M, Rossomacha E, Sun J, Chevrier A, Shive MS, *et al*. Chitosan-glycerol phosphate/blood implants improve hyaline cartilage repair in ovine microfracture defects. J Bone Joint Surg Am 2005;8(12):2671–86.
16. Hoemann CD, Sun J, McKee MD, Chevrier A, Rossomacha E, Rivard GE, *et al*. Chitosan-glycerol phosphate/blood implants elicit hyaline cartilage repair integrated with porous subchondral bone in microdrilled rabbit defects. Osteoarthritis Cartilage 2007;15(1):78–89.
17. Hoemann CD, Chen G, Marchand C, Tran-Khanh N, Thibault M, Chevrier A, *et al*. Scaffold-guided subchondral bone repair: implication of neutrophils and alternatively activated arginase-1+ macrophages. Am J Sports Med 2010;38(9):1845–56.
18. Mackie EJ, Ahmed YA, Tatarczuch L, Chen KS, Mirams M. Endochondral ossification: how cartilage is converted into bone in the developing skeleton. Int J Biochem Cell Biol 2008;40(1):46–62.
19. Vortkamp A, Pathi S, Peretti GM, Caruso EM, Zaleske DJ, Tabin CJ. Recapitulation of signals regulating embryonic bone formation during postnatal growth and in fracture repair. Mech Dev 1998;71(1–2):65–76.
20. Hunziker EB. Mechanism of longitudinal bone growth and its regulation by growth plate chondrocytes. Microsc Res Tech 1994;28(6):505–19.
21. Hunziker EB, Schenk RK, Cruz-Orive LM. Quantitation of chondrocyte performance in growth-plate cartilage during longitudinal bone growth. J Bone Joint Surg Am 1987;69 (2):162–73.
22. Archer CW, Morrison H, Pitsillides AA. Cellular aspects of the development of diarthrodial joints and articular cartilage. J Anat 1994;184(Pt 3):447–56.
23. Hayes AJ, MacPherson S, Morrison H, Dowthwaite G, Archer CW. The development of articular cartilage: evidence for an appositional growth mechanism. Anat Embryol (Berl) 2001;203(6):469–79.
24. Hunziker EB, Kapfinger E, Geiss J. The structural architecture of adult mammalian articular cartilage evolves by a synchronized process of tissue resorption and neoformation during postnatal development. Osteoarthritis Cartilage 2007;15(4): 403–13.
25. Ferguson C, Alpern E, Miclau T, Helms JA. Does adult fracture repair recapitulate embryonic skeletal formation? Mech Dev 1999;87(1–2):57–66.
26. Gerstenfeld LC, Cullinane DM, Barnes GL, Graves DT, Einhorn TA. Fracture healing as a post-natal developmental process: molecular, spatial, and temporal aspects of its regulation. J Cell Biochem 2003;88(5):873–84.
27. Maeda Y, Nakamura E, Nguyen MT, Suva LJ, Swain FL, Razzaque MS, *et al*. Indian Hedgehog produced by postnatal chondrocytes is essential for maintaining a growth plate and trabecular bone. Proc Natl Acad Sci U S A 2007;104(15): 6382–7.
28. Hooper JE, Scott MP. The Drosophila patched gene encodes a putative membrane protein required for segmental patterning. Cell 1989;59(4):751–65.
29. Ingham PW, Taylor AM, Nakano Y. Role of the Drosophila patched gene in positional signalling. Nature 1991;353 (6340):184–7.
30. Chen H, Sun J, Hoemann CD, Lascau-Coman V, Ouyang W, McKee MD, *et al*. Drilling and microfracture lead to different bone structure and necrosis during bone-marrow stimulation for cartilage repair. J Orthop Res 2009;27(11):1432–8.
31. Chevrier A, Rossomacha E, Buschmann MD, Hoemann CD. Optimization of histoprocessing methods to detect glycosaminoglycan, collagen type I and collagen type II in decalcified rabbit osteochondral sections. J Histotechnol 2005;28:165–75.
32. Baumgartner L, Arnhold S, Brixius K, Addicks K, Bloch W. Human mesenchymal stem cells: influence of oxygen pressure on proliferation and chondrogenic differentiation in fibrin glue in vitro. J Biomed Mater Res A 2010;93(3):930–40.
33. Kratzel C, Bergmann C, Duda G, Greiner S, Schmidmaier G, Wildemann B. Characterization of a rat osteotomy model with impaired healing. BMC Musculoskelet Disord 2008;8 (9):135–47.
34. Naik AA, Xie C, Zuscik MJ, Kingsley P, Schwarz EM, Awad H, *et al*. Reduced COX-2 expression in aged mice is associated

with impaired fracture healing. J Bone Miner Res 2009;24 (2):251–64.
35. Gurtner GC, Werner S, Barrandon Y, Longaker MT. Wound repair and regeneration. Nature 2008;453(15):314–21.
36. Grant WT, Wang GJ, Balian G. Type X collagen synthesis during endochondral ossification in fracture repair. J Biol Chem 1987;262(20):9844–9.
37. Brown WE, Potter HG, Marx RG, Wickiewicz TL, Warren RF. Magnetic resonance imaging appearance of cartilage repair in the knee. Clin Orthop Relat Res 2004;422:214–23.
38. Minas T, Gomoll AH, Rosenberger R, Royce RO, Bryant T. Increased failure rate of autologous chondrocyte implantation after previous treatment with marrow stimulation techniques. Am J Sports Med 2009;37(5):902–8.